research article

Adnexal masses characterized on 3 tesla magnetic resonance imaging – added value of diffusion techniques

Julia Dimova[1], Dora Zlatareva[1], Rumiana Bakalova[2,3,4], Ichio Aoki[3,4], George Hadjidekov[2,5]

[1] Department of Diagnostic Imaging, Medical University, Sofia, Bulgaria
[2] Department of Physics, Biophysics and Radiology, Sofia University "St. Kliment Ohridski", Sofia, Bulgaria
[3] Department of Molecular Imaging and Theranostics and
[4] Group of Quantum-state Controlled MRI, National Institutes for Quantum and Radiological Science and Technology (QST/NIRS), Chiba, Japan
[5] Department of Radiology, University Hospital "Lozenetz", Sofia, Bulgaria

Radiol Oncol 2020; 54(4): 419-428.

Received 19 June 2020
Accepted 14 September 2020

Correspondence to: Prof. George Hadjidekov, M.D., University Hospital Lozenetz, Department of Radiology, Koziak 1 str. 1407 Sofia, Bulgaria, E-mail: jordiman76@yahoo.com

Disclosure: No potential conflicts of interest were disclosed.

Background. To assess different types of adnexal masses as identified by 3T MRI and to discuss the added value of diffusion techniques compared with conventional sequences.

Patients and methods. 174 women age between 13 and 87 underwent an MRI examination of the pelvis for a period of three years. Patients were examined in two radiology departments – 135 of them on 3 Tesla MRI Siemens Verio and 39 on 3 Tesla MRI Philips Ingenia. At least one adnexal mass was diagnosed in 98 patients and they are subject to this study. Some of them were reviewed retrospectively. Data from patients' history, physical examination and laboratory tests were reviewed as well.

Results. 124 ovarian masses in 98 females' group of average age 47.2 years were detected. Following the MRI criteria, 59.2% of the cases were considered benign, 30.6% malignant and 10.2% borderline. Out of all masses 58.1% were classified as cystic, 12.9% as solid and 29% as mixed. Of histologically proven tumors 74.4% were benign and 25.6% were malignant. All of the malignant tumors had restricted diffusion. 64 out of all patients underwent contrast enhancement. (34 there were a subject of contraindications). 39 (61%) of the masses showed contrast enhancement.

Conclusions. Classifying adnexal masses is essential for the preoperative management of the patients. 3T MRI protocols, in particular diffusion techniques, increase significantly the accuracy of the diagnostic assessment.

Key words: adnexal masses; 3 Tesla MRI; diagnosis; malignancy; ovarian neoplasms; diffusion restriction

Introduction

Incidental adnexal masses are commonly detected in daily medical practice due to the frequent lack of clinical manifestation.[1] Approximately 9% to 10% of women undergoing ultrasound have ovarian lesions.[2] Although most commonly used, ultrasound has some limitations including the small field of view, low resolution and interference by obesity or by gaseous bowel loops.[3] Ultrasound indeterminate adnexal masses vary between 5% and 25%.[4,5] If furthermore examined with computed tomography (CT), distant metastases, respectively the staging of the disease could be assessed. Magnetic resonance (MR) has been considered as the most useful imaging technique for characterizing adnexal formations. This modality has a key role in the preoperative evaluation and their follow-up, identifying the origin of the mass and the different types of tissue contained in with accuracy of 88% to 93%.[6] 3 Tesla MRI is superior for examining female pelvis due to its higher resolution and the possibil-

ity of providing more detailed images.[7-9] MRI techniques such as diffusion-weighted imaging (DWI) and apparent diffusion coefficient (ADC) are of an additional benefit differentiating malignant from benign lesions.[10-12]

The aim of our study is to assess different types of adnexal masses as identified by 3T MRI and to discuss the added value of diffusion and perfusion techniques compared with conventional sequences.

Patients and methods

174 women age between 13 and 87 underwent MRI examination of the pelvis for a period of three years. Indications were: sonographically detected pelvic mass; or gynecological complaints; or history of previous adnexal tumor; or family history of ovarian cancer. Six women were examined for other reasons (hips, sigma/colon or perianal abscess), nine for uterine pathology, but adnexal mass was detected and the complete gynecological MRI protocol was performed, too. At least one adnexal mass was diagnosed in 98 patients and they are subject of this study. 51% of them were reviewed retrospectively. Data from patients' history, physical examination and laboratory tests were reviewed as well.

Patients were examined in two radiology departments, 135 of them on 3 Tesla MRI Siemens Verio and the 39 on 3 Tesla MRI Philips Ingenia. The Siemens MRI protocol included: coronal (COR) T1; sagittal (SAG) T2; paracoronal and paratransversal of the uterus T2 with and without fat saturation; SAG T1; transversal T1 Vibe Dixon; DWI and ADC. The Philips MRI protocol included: COR STIR; SAG T2; COR T2; COR T1; axial (AX) T2; AX T2 with fat saturation; DWI and ADC. (Table 1)

Measurement of the ADC value was carried out for all ovarian masses in our study. For each tumor a region of interest (ROI: 1 cm^2) was manually defined. In the mixed malignant formations ROIs were placed on the solid component only. The ADC values are presented as numerical value x 10^{-3} mm^2/s representing quantitative metric.

Intravenous contrast administration was applied when needed and when there were no contraindications. A macrocyclic contrast agent Gadobutrol [1.0 mmol/ml] (Gadovist® 1.0, Bayerhealthcare, Berlin, Germany) was used at a dose of 0.1 mmol/kg in all contrast-enhanced studies on both MR devices. Injection rate of 0.5 mL/sec was performed in order to achieve equimolar amounts of gadolinium. Saline flush (25–30 ml) at the same flow rate followed the contrast administration.

In part of our cases dynamic contrast enhanced – magnetic resonance imaging (DCE-MRI) was performed and time-signal intensity curve (TIC) was generated using the Mean Curve software package (Philips). A round region of interest (ROI: 1 cm^2) was placed at target areas referring to T2W and contrast-enhanced images. Areas with hemorrhage and necrosis were avoided.

The following patterns were evaluated on MR images:
- tumor appearance (cystic, solid or mixed)
- uni- or bilateral ovaries involvement
- size of the mass
- adipose tissue presence or not
- signal intensity on T2 weighted images
- diffusion restriction
- wall thickness
- presence or not of septa
- papillary projections
- presence or not of ascites
- lymph nodes involvement and metastases

Following MR criteria of malignancy, as reported in the literature (by Jeong *et al*.[13], Valentini *et al*.[6] and El-Wekil *et al*.[14]), are used:
- lesion size more than 4 cm
- solid components with heterogeneous enhancement
- papillary projections
- septa thick more than 3 mm
- areas of necrosis and breaking down
- lymph nodes involvement sized more than 1 cm.

SPSS Statistics release 21 for Microsoft Windows was used to perform Kolmogorov-Smirnov (2-tailed) test for establishing correlations between malignancy and diffusion restriction and between malignancy and type of mass.

Approval was obtained from the Institutional Review Board of both University hospitals prior the initiation of the study. Informed written consent was obtained from each patient. Personal identity information of all patients was protected.

Results

In 98 females of average age 47.2 years, a total of 124 ovarian masses were detected. In 16 of the patients (16.3%) additional uterine pathology was found. One case considered as an ovarian cyst was histologically proven to be an inclusion peritoneal

TABLE 1. 3 Tesla Siemens and 3 Tesla Philips MRI protocols

	FOV (mm)	Matrix (mm)	Slice thickness (mm)	TR (ms)	TE (ms)	Voxel size (mm)	TA (min)
SIEMENS VERIO 3.0T							
T1 COR	300	390/320	5	500	8.7	0.9×0.9×5.0	01:36
T2 SAG	200	320/320	4	3300	133	0.6×0.6×4.0	03:44
T2 paracor	200	320/320	4	3700	140	0.6×0.6×4.0	03:24
T2 paracor +FS	200	256/256	4	3700	131	0.8×0.8×4.0	01:58
T2 paratra	200	320/320	4	3740	148	0.6×0.6×4.0	03:29
T2 paratra + FS	200	256/256	4	3700	138	0.8×0.8×4.0	02:13
T1 SAG	160	217/192	4	569	12	0.4×0.4×4.0	03:44
T1 vibe dixon AX	380	188/320	3.5	3.92	1.27	0.6×0.6×3.5	00:19
DWI AX (b50-400-800)	360	100/128	5	4700	57	1.4×1.4×5.0	02:49
POST C							
T1 vibe dixon AX	380	188/320	3.5	3.92	1.27	0.6×0.6×3.5	00:19
T1 SAG	160	217/192	4	569	12	0.4×0.4×4.0	03:44
T1 COR	300	390/320	5	500	8.7	0.9×0.9×5.0	01:36
PHILIPS INGENIA 3.0T							
COR STIR	340	228/186	5	5622	50	1.5×1.5×5.0	03:45
T2 SAG	229	208/208	3	3776	100	1.1×1.1×3.0	03:01
COR T2	315	392/297	5	4846	90	0.8×1.6×5.0	01:56
COR T1	315	392/315	5	483	8	0.8×1.2×5.0	02:11
AX T2	261	328/251	5	4805	100	0.8×1.0×5.0	02:05
AX T2 FS	261	236/208	5	4346	80	1.11×1.25×5.0	02:37
DWI 3b 0,100,800	375	124/106	4	5299	77	3.0×3.0×4.0	01:51
POST C							
MDixon AX	240	220/222	3,5	5.4	1.96	1.09×1.08×3.5	02:58
COR T1 FS	315	392/309	5	519	8	0.8×1.02×5.0	02:17

AX = axial; COR = coronal; COR STIR = coronal short tau inversion recovery; DWI = diffusion-weighted imaging; FS = fat sat; paracor = paracoronal; SAG = sagital

cyst. The results of all ovarian masses according to their MRI features are listed in Table 2.

Following the MRI criteria, 59.2% of the cases were considered benign, 30.6% malignant and 10.2% borderline. The results of DWI sequences show a statistically significant correlation with the assessment of masses as benign/borderline/malignant. 34.3% of all malignant cases were found in the age group 61–70. Of all patients 32 were tested for CA-125 tumor marker and 12 had elevated levels. Only half of those 12 cases were histologically proven malignant.

The biggest diameter of all 124 ovarian masses was measured – the largest one was 216 mm, the smallest one was under 10 mm. 54% of all tumors had diameter larger than 4 cm.

58.1% out of all masses were classified as cystic, 12.9% as solid and 29% as mixed. In four cases both solid and cystic masses were found in the same patient. Of all ovarian tumors 37 (29.8%) had wall thickness greater than 3 mm, 16 (12.9%) had papillary projections and 41 (33%) were septated. Only 6 masses of all contained fat, 5 of them were histologically proven to be mature teratomas. Kolmogorov-Smirnov test shows a statistically significant correlation between the type of mass and the assessment of masses as benign/borderline/malignant.

Of histologically proven tumors 74.4% were benign and 25.6% were malignant. All masses classified on MRI as benign were identified correctly. Two masses, described as suspicious and malignant, turned out to be benign. All of the malignant

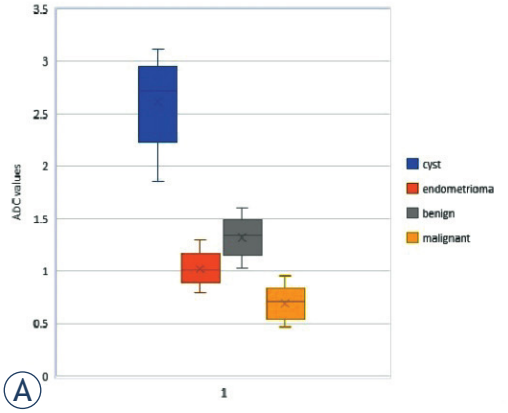

A

ADC values ($\times 10^{-3}$ mm^2/s) benign	malignant
2.72 ± 0.10	0.66 ± 0.23
1.34 ± 0.09	0.89 ± 0.12
3.04 ± 0.02	1.09 ± 0.15
1.01 ± 0.05	0.71 ± 0.03
0.80 ± 0.04	0.98 ± 0.05
0.61 ± 0.06	1.06 ± 0.10
2.07 ± 0.44	0.82 ± 0.06
1.55 ± 0.12	0.67 ± 0.18
2.50 ± 0.08	0.91 ± 0.32
2.61 ± 0.11	0.60 ± 0.15
1.03 ± 0.38	0.7 ± 0.06
2.64 ± 0.32	0.96± 0.10

B

FIGURE 1. (A) Box plot presenting ADC values in four different types of adnexal tumors – highest ADC value found in a simple cyst; lowest found in a malignant tumor. **(B)** Mean apparent diffusion coefficient (ADC) values of twelve patients with histologically proven benign adnexal lesion and twelve patients with histologically proven malignant adnexal lesion. All values are expressed as mean value ± standard deviation (SD) x 10 $^{-3}$ mm 2 /s.

tumors had restricted diffusion. The calculated ADC values of malignant adnexal masses are significantly lower than the ADC values of benign masses. Exceptions were found for endometrioma (1.01 ± 0.05 x 10^{-3} mm^2/s); mature teratoma (0.80 ± 0.04 x 10–3 mm2/s) and chronic abscess (0.61 ± 0.06 x 10^{-3} mm^2/s) – all of them presenting lower ADC values. (Figure 1) 72.7% of malignant neoplasms were mixed masses, 18.2% were solid and only one (9.1%) was cystic. Compared to them, 75% of benign tumors were cystic.

64 out of all 98 patients underwent contrast enhancement. 34 there were a subject of contraindications (history of previous allergic reactions to the contrast agent, elevated levels of serum creatinine or patient refusal). 39 (61%) of the masses showed enhancement. Three were classified as benign and four – as suspicious. 32 of the enhanced tumors were identified as malignant.

Ascites was found in 33 of the cases – in 15 of which is located only in the pouch of Douglas. In 15.3% of the cases, enlarged lymph nodes with diffusion restriction were found – all in patients with malignant masses and one with a proven chronic inflammatory process. In 15 cases enlarged metastatic locoregional lymph nodes were found. Eight patients had peritoneal deposits; four patients liver metastases; three patients bone metastases, two patients were with urinary bladder invasion and one patient had adrenal metastasis. In all cases with metastases three turned out to be from uterine cancer (ovarian masses in these cases were proven benign).

TABLE 2. Results of 124 ovarian masses according to their MRI features

	Malignant	Benign	Borderline
Cystic masses	5/41 *(12.2%)*	61/71 *(85.9%)*	6/12 *(50%)*
Solid masses	10/41 *(24.4%)*	4/71 *(5.6%)*	2/12 *(16.6%)*
Mixed masses	26/41 *(63.4%)*	6/71 *(8.5%)*	4/12 *(33.4%)*
Cases with one ovary involvement	18/30 *(60%)*	46/58 *(79.3%)*	9/10 *(90%)*
Cases with both ovaries' involvement	12/30 *(40%)*	12/58 *(20.7%)*	1/10 *(10%)*
Size of the mass (more than 4 cm)	37/41 *(90.2%)*	22/71 *(31%)*	8/12 *(66.7%)*
Masses with adipose tissue presence	-	5/71 *(7%)*	1/12 *(8.3%)*
Masses with high signal intensity in T2WI	5/41 *(12.2%)*	42/71 *(59.1%)*	5/12 *(41.6%)*
Masses with low signal intensity in T2WI	7/41 *(17.1%)*	18/71 *(25.4%)*	1/12 *(8.4%)*
Heterogeneous masses	29/41 *(70.7%)*	11/71 *(15.5%)*	6/12 *(50%)*
Diffusion restriction	39/41 *(95.1%)*	19/71 *(26.8%)*	7/12 *(58.4%)*
Wall thickness (more than 3 mm)	20/41 *(48.8%)*	12/71 *(16.9%)*	5/12 *(41.7%)*
Presence of septa	25/41 *(61%)*	11/71 *(15.5%)*	5/12 *(41.7%)*
Papillary projections presented	14/41 *(34.1%)*	-	2/12 *(16.6%)*
Cases with presence of ascites	16/30 *(53.3%)*	15/58 *(25.9%)*	2/10 *(20%)*
Lymph nodes involvement and metastases	20/30 *(66.6%)*	3/58* *(5.2%)*	1/10 *(10%)*

T2WI = T2 weighted imaging

Discussion

Assessing different types of adnexal lesions is important preoperatively. We find a number of reasons about the value of 3 Tesla MRI in such differentiation.

The MRI gynecological protocols we used concur the ESUR Quick Guide to Female Pelvis

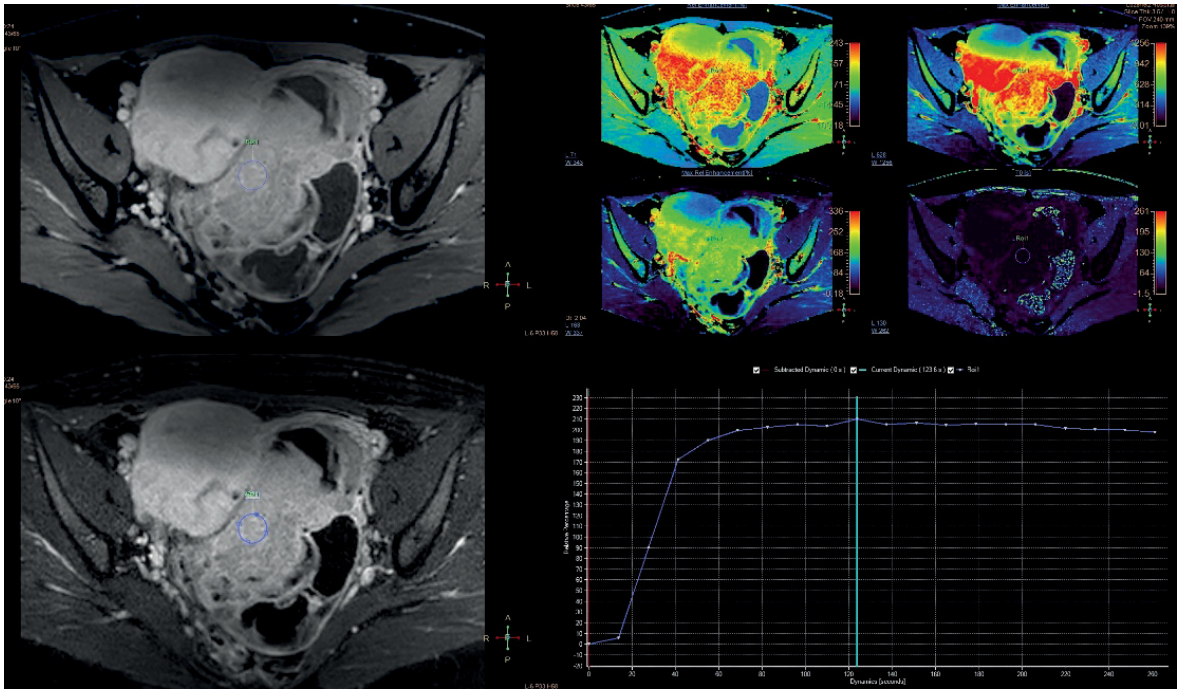

FIGURE 2. Type III time intensity curve (TIC) of a malignant adnexal mass.

Imaging, 1.0 from 2019.[15] Classical sequences (T1, T2) combined with post-gadolinium sequences and diffusion techniques provide reliable information on the nature of the adnexal masses.

It is known from previous studies that dynamic contrast enhanced MRI (DCE-MRI) is helpful in characterizing adnexal tumors. It could discriminate malignant from benign masses. According to the study of Thomassin-Naggara *et al.* there are three types of TIC showing benign, borderline and malignant ovarian tumors. Figure 2 demonstrates representative Type III curve of a malignant adnexal mass.

The number of patients (98) in our study exceeds those of similar ones known from the literature (30 in El-Wekil *et al*.[14] and 58 in Koc *et al*.[16]). The average age of patients (47.2 years) as well differs respectably by seven and four years from the cited studies.[14,16]

The WHO histological classification (according to Foti *et al*.[17]) divides primary ovarian masses into three main categories: epithelial, germ cell and sex cord-stromal tumors. Metastatic tumors are classified in a separate category. In 2016 Meinhold-Heerlein *et al.* revised the WHO classification introducing seromucinous tumors as a new entity.[18] Our study includes 14 histologically different groups of ovarian masses – ten benign and four malignant. Diffusion MRI appearance of histologically different groups is shown in Table 3. Some of the benign formations have diffusion restriction – abscess, endometrioma, mature cystic teratoma

TABLE 3. Diffusion MRI appearance of histologically different groups

Histopathological findings	DWI restricted	DWI Facilitated
Simple cyst	-	5
Inclusion cyst	-	1
Abscess	1	-
Endometrioma	12	5
Teratoma	5	-
Serous cystadenoma	-	2
Mucinous cystadenoma	1	1
Serous adenofibroma	1	-
Serous cystadenofibroma	1	-
Brenner tumor	-	1
Seromucinous carcinoma	2	-
Serous papillary adenocarcinoma	2	-
Adenosarcoma	1	-
Metastases	6	-

DWI = diffusion-weighted imaging

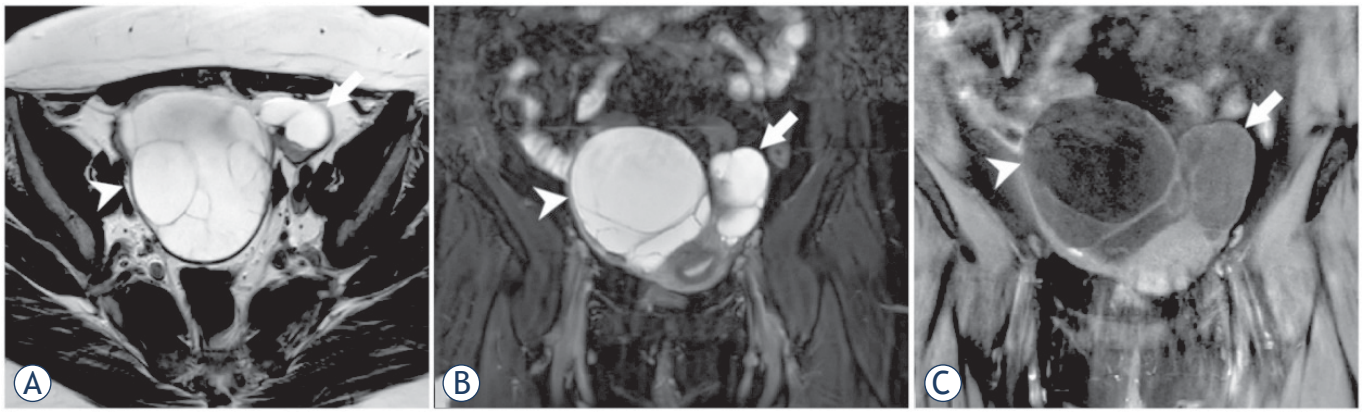

FIGURE 3. 45-year old patient with bilateral adnexal masses; serous papillary cystadenoma (arrow) and mucinous cystadenoma (arrowhead); both masses have predominantly high signal intensity on T2WI and T2WI fat sat **(A)**, **(B)** and low signal intensity on T1WI fat sat **(C)**.

and serous adenofibroma. In 88% of cases mature cystic teratomas are filled with sebaceous material and are lined with keratinized squamous epithelium[19], compared to the most relevant feature – adipose tissue which is presented in only 67–75%.[20] Diffusion restriction is caused by the presence of keratin or Rokitansky nodule and fat globules.[21] Endometriomas as containing blood and hemosiderin can show diffusion restriction too.[21,22] Solid areas with similar changes can help the detection of malignant transformation. When it comes to an ovarian abscess, diffusion characteristics depend on the content – in more viscous one the signal intensity is higher on DWI and lower on ADC map.[23] Diffusion techniques could differentiate abscess from cystic or necrotic neoplasm. Neoplasms usually show diffusion restriction peripherally and abscesses centrally.[22,24] According to cystic degeneration, some adenofibromas also could be characterized by restriction of the water molecules.[22,25,26]

In this study adnexal masses are classified based on their morphological appearance, similar to Foti *et. al.*[17] and divided into three main groups – cystic, solid and mixed (cystic and solid).

Cystic adnexal masses could be unilocular or multilocular. Some of them have a non-ovarian origin. They are usually benign, with low signal intensity on T1-weighted images and high signal intensity on T2-weighted images.

Peritoneal inclusion cysts and hydrosalpinx are the most common extra ovarian lesions. They occur almost exclusively in premenopausal women and at imaging the ovaries are clearly separated from these cystic formations.[27,28]

Functional ovarian cysts are the most common finding in women of reproductive age. Follicles are up to 20 mm as the dominant one could be 25 mm. Follicular cysts and corpus luteum cysts are larger and tend to increase if there is internal bleeding. This manifests with an increase of the signal on

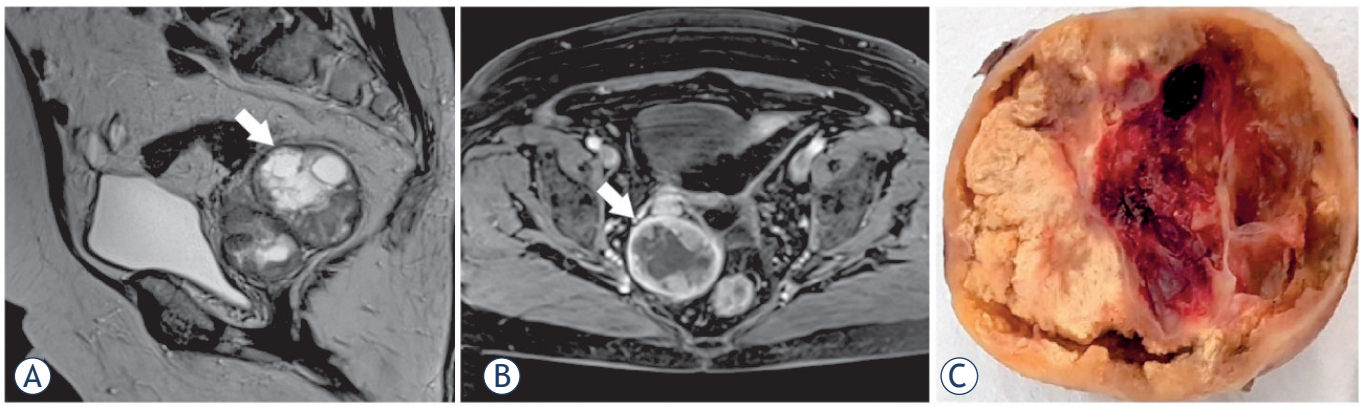

FIGURE 4. 68-year old patient with previous hysterectomy; right serous cystadenofibroma (arrow); complex mass - heterogeneous on T2WI **(A)** which shows peripheral enhancement on T1WI fat sat with contrast **(B)**. **(C)** Macroscopic histological preparation of the tumor.

T1-weighted images.[13,17] They do not usually have diffusion restriction and does not change after contrast administration. Although, in corpus luteum cysts intense wall enhancement may be seen.

Serous cystadenoma and mucinous cystadenoma are benign tumors with thin walls (Figure 3). Mucinous type is usually larger, septated and has variable intensity on both T1- and T2-weighted images based on different mucin concentration. Some loculi are hyperintense on T1-weighted images, forming a pattern known as "honeycomb" or "stained glass".[17,29,30] Serous cystadenoma is more often bilateral and its wall could contain small nodules due to fibrosis or calcification.[31,32] Diffusion restriction could be detected in mucinous cystadenoma due to the dense mucinous material.[12]

Cystadenofibroma is usually a benign epithelial tumor that can present as a complex cystic mass with thick septa and solid component. It could present with plaques and nodules that have low signal intensity on T2-weighted images due to fibrous tissue (Figure 4).[33-35]

Endometriomas are part of the cystic lesions containing blood products. In addition to that, they characterize with hyperintensity on T1-weighted images and lower signal intensity on T2-weighted images, called "shading sign". Sometimes these lesions could have high signal intensity on both T1- and T2-weighed images. They do not change their signal intensity on fat-suppressed sequences.[13,31,36,37] Patients having endometriosis are at risk of developing ovarian malignancies.[38] Endometriomas usually do not enhance after contrast administration but could have restricted diffusion.[11,22]

Mixed ovarian masses containing both cystic and solid parts are always suspicious for malignant – surface epithelial tumors and metastases. The benign representative of this category is mature cystic teratoma.

Mature cystic teratoma is known as the most common ovarian neoplasm that arises from ovarian germ cells.[13,31] Usually part of this tumor has high signal intensity on T1WI and intermediate on T2WI, fat-fluid or fluid-fluid level, low signal calcification parts and floating debris. It could also have a soft-tissue protuberance called Rokitansky nodule. On fat-suppressed sequences the areas containing fat show drop in signal intensity. Malignant transformation of mature cystic teratoma is rare.[19,37,39,40] Enhancement after contrast application is not typical. They could represent with restricted diffusion in the areas with keratin and fat globules.[22,23]

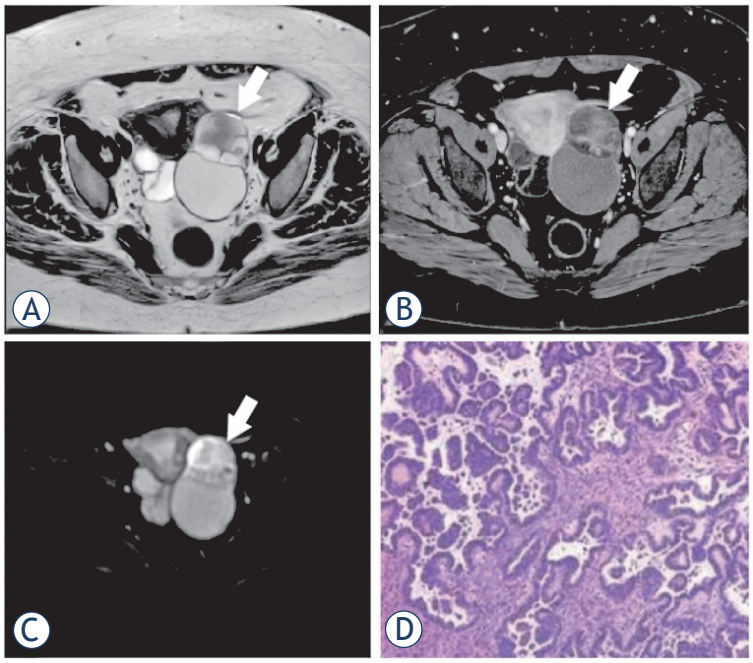

FIGURE 5. 57- year old patient with left serous papillary adenocarcinoma (arrow); predominantly cystic mass with high signal intensity on T2WI **(A)** and solid component which is enhanced on T1WI fat sat with contrast **(B)**. Part of the mass characterizes with diffusion restriction **(C)**. **(D)** Microscopy preparation of the tumor.

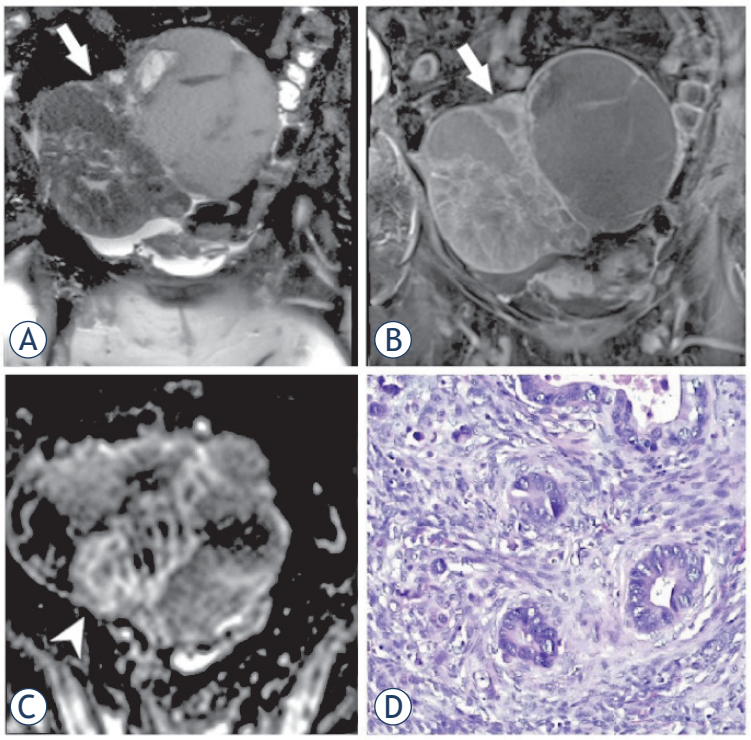

FIGURE 6. 63- year old patient with right ovarian metastasis from adenocarcinoma with intestinal phenotype; complex septated mass with heterogeneous signal intensity on T2WI **(A)**; enhancement mostly in wall and septi on T1WI fat sat with contrast **(B)**; part of the mass (arrowhead) has restricted diffusion; **(D)** Microscopy preparation of the metastasis.

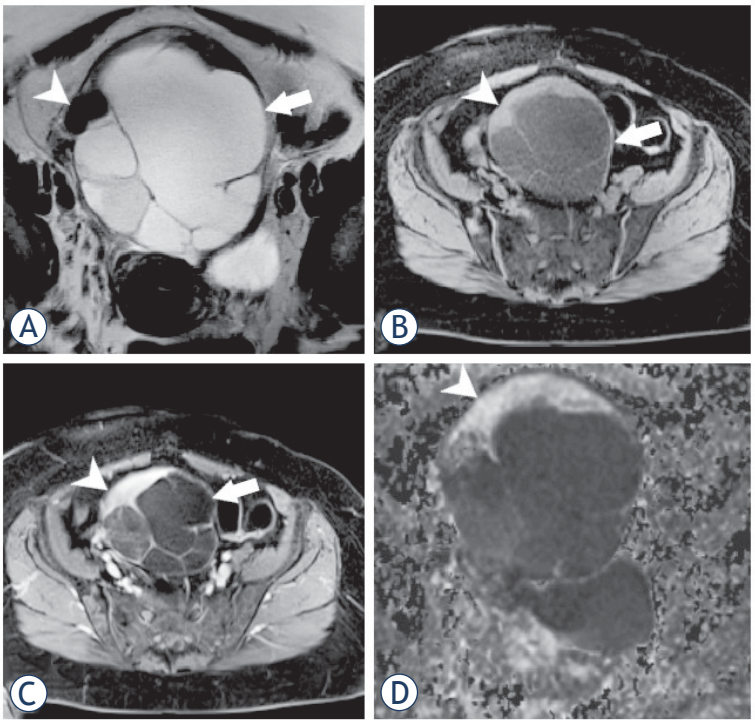

FIGURE 7. 54- year old patient with mucinous cystadenoma (arrow) coexisting with benign Brenner tumor (arrowhead); mucinous cystadenoma has high signal intensity on T2WI **(A)** and low on T1WI fat sat **(B)**; compared to it Brenner tumor has low signal intensity on T2WI **(A)** and high on T1WI fat sat **(B)**; on T1 fat sat with contrast **(C)** only Brenner tumor shows enhancement and on DWI **(D)** only Brenner tumor shows restricted diffusion.

Serous and mucinous cystadenocarcinoma are the most common epithelial malignancies of the ovaries – 50% and 10% of malignant lesions.[41] Mucinous tumors are larger, lobulated and may be hyperintense on T1WI in addition to the high protein concentration in mucoid material.[30,42] Cystadenocarcinomas have thick and irregular walls, septations, solid components and papillary projections that have low signal intensity on T2WI with contrast enhancement after contrast administration. Serious fluid part demonstrates with high signal intensity on T2WI (Figure 5). Peritoneal invasion is sometimes discovered.[17,41] In connection with their malignant nature, a pronounced diffusion restriction is observed.

Ovarian metastases most frequently originate from a primary process in the female genital tract, gastrointestinal tract (Krukenberg tumor) or breast. They are more commonly bilateral and multiloculated. Their solid parts are hypointense on T2WI and enhance after gadolinium administration. Distinguishing them from a primary ovarian process is not easy.[17,41,43] Ovarian metastases have high signal intensity on DWI and low on ADC map (Figure 6).

Other less common representatives of mixed ovarian neoplasms are endometrioid tumors, yolk sac tumors and granulosa cell tumors.

Solid ovarian masses could have benign, borderline and malignant behavior. They include all three main histological types – epithelial, germ cell and sex cord tumors and metastases.

The Brenner tumor is a rare epithelial tumor and represents 2% of ovarian neoplasms.[44] It is usually benign and has largely homogeneous low signal intensity on T1- and T2-weighed images. Its signal intensity is similar to those of fibromas but no cysts and necrosis are found in Brenner tumor. This ovarian tumor can occur in association with mucinous cystadenoma (Figure 7). Mild enhancement is observed after contrast application. Diffusion restriction is not characteristic of benign representatives of this tumor.[39,45]

Fibromas encounter around 4% of all ovarian tumors. They could mimic malignant neoplasm as their size can vary and may be associated with ascites and pleural effusion (Meig syndrome). Another pathology they should be defined from is pedunculated uterine leiomyoma. These tumors demonstrate low signal intensity on both T1- and T2-weighted images. Scattered areas of high signal intensity could be present on T1WI due to cystic degeneration or edema.[13,17,35] In this case diffusion restriction may be found. After contrast administration minimal enhancement is evident.

In this study 72.7% of histologically proven malignant neoplasms were mixed cystic and solid, 18.2% were solid and only one (9.1%) was cystic. That statement disagrees with El-Wekil *et al*.[14] where no solid mass was found but cystic masses were 37.5% of their case series. However, 62.5% of tumors in their study were mixed cystic and solid which roughly coincides with our findings.

All of the histologically proven malignant lesions in this study show restricted diffusion. This confirms the literature data that an adnexal mass with higher signal intensity on DWI and lower on ADC map usually is a malignant lesion. Our results confirm the findings of previous studies in the literature that benign adnexal lesions have higher ADC values than the malignant once. We also found some exceptions of this statement concerning endometrioma, mature teratoma and chronic abscess presenting with lower ADC values despite of their benign origin.

Borderline ovarian tumors are usually complex masses that have some of the MR characteristics of

the malignant one. They could show cellular proliferation and moderate nuclear atypia but without stromal invasion.[46,47] Similar to the study of Bent *et. al.*[46] we identified 11 of the cases as suspicious. All of them demonstrated one or more MRI feature suggestive for malignancy – size more than 4 cm, solid part, cystic part with vegetations and septations, wall thickness more than 3 mm; contrast enhancement. In our study only one of the 10 suspicious cases were bilateral.

CA-125 is established tumor marker for ovarian cancer.[13,48] Limitation of this study is the small number of CA-125 tests performed before magnetic resonance imaging. Of these, elevated levels of CA-125 were found in 12 patients. Similarly, to other studies, over 60% of our patients with elevated CA-125 levels have proven malignant ovarian lesions.

Concerning unilateral or bilateral adnexal masses, we found malignant to be more often bilateral. Unilateral lesions are more often found in the right adnexa and in younger patients. This study as well as the Zhang *et al.* one[49] suggests that large sizes and atypical signal intensity may influence the correct assessment of the type of ovarian lesions. The main limitations of our study include the retrospective reviewing of patients with some clinical missing, as well as surgical missing findings in patients who underwent surgery in another hospital.

Conclusions

Classifying adnexal masses is essential for the preoperative management of the patients. 3T MRI protocols, in particular diffusion techniques, increase significantly the accuracy of the diagnostic assessment. Further studies correlated with histological validation would support the role of MRI as a mandatory part of the patients' management.

Acknowledgements

This study was partially supported by the Japanese Society for the Promotion of Science (JSPS) (Grand-in-aid "Kakenhi C" granted to R.B. and the Japanese Agency for Medical Research and Development (AMED) (Project for Cancer Research and Therapeutic Evolution, P-CREATE, no. 16 cm0106202h0001).

References

1. Expert Panel on Women's Imaging, Atri M, Alabousi A, Reinhold C, Akin EA, Benson CB, Bhosale PR, et al. ACR Appropriateness Criteria® clinically suspected adnexal mass, no acute symptoms. *J Am Coll Radiol* 2019; **16:** S77-93. doi: 10.1016/j.jacr.2019.02.011
2. Sharma A, Apostolidou S, Burnell M, Campbell S, Habib M, Gentry-Maharaj A, et al. Risk of epithelial ovarian cancer in asymptomatic women with ultrasound-detected ovarian masses: a prospective cohort study within the UK collaborative trial of ovarian cancer screening (UKCTOCS). *Ultrasound Obstet Gynecol* 2012. **40:** 338-44. doi: 10.1002/uog.12270
3. Biggs WS, Marks ST. Diagnosis and management of adnexal masses. *Am Fam Physician* 2016; **93:** 676-81. PMID: 27175840
4. Van Calster B, Timmerman D, Valentin L, McIndoe A, Ghaem-Maghami S, Testa AC, et al. Triaging women with ovarian masses for surgery: observational diagnostic study to compare RCOG guidelines with an International Ovarian Tumour Analysis (IOTA) group protocol. *BJOG* 2012; **119:** 662-71. doi: 10.1111/j.1471-0528.2012.03297.x
5. Thomassin-Naggara I, Poncelet E, Jalaguier-Coudray A, Guerra A, Fournier LS, Stojanovic S, et al. Ovarian-adnexal reporting data system magnetic resonance imaging (O-RADS MRI) score for risk stratification of sonographically indeterminate adnexal masses. *JAMA Netw Ope*n 2020; **3:** e1919896. doi: 10.1001/jamanetworkopen.2019.19896
6. Valentini AL, Gui B, Miccò M, Mingote MC, De Gaetano AM, Ninivaggi V, et al. Benign and suspicious ovarian masses-MR imaging criteria for characterization: Pictorial review. *J Oncol* 2012; **2012:** 481806. doi: 10.1155/2012/481806
7. Kataoka M, Kido A, Koyama T, Isoda H, Umeoka S, Tamai K, et al. MRI of the female pelvis at 3T compared to 1.5T: evaluation on high-resolution T2-weighted and HASTE images. *J Magn Reson Imaging* 2007; **25:** 527-34. doi: 10.1002/jmri.20842
8. Léautaud A, Marcus C, Ben Salem D, Bouché O, Graesslin O, Hoeffel C. *Pelvic MRI at 3.0 Tesla. J Radiol* 2009; **90:** 277-86. doi: 10.1016/s0221-0363(09)72506-5
9. Hussain SM, van den Bos IC, Oliveto JM, Martin DR. MR imaging of the female pelvis at 3T. *Magn Reson Imaging Clin N Am* 2006; **14:** 537-44, vii. doi: 10.1016/j.mric.2007.01.008
10. Thomassin-Naggara I, Balvay D, Rockall A, Carette MF, Ballester M, Darai E, et al. Added value of assessing adnexal masses with advanced MRI techniques. *Biomed Res Int* 2015; **2015:** 785206. doi: 10.1155/2015/785206
11. Davarpanah AH, Kambadakone A, Holalkere NS, Guimaraes AR, Hahn PF, Lee SI. Diffusion MRI of uterine and ovarian masses: identifying the benign lesions. *Abdom Radiol* 2016; **41:** 2466-75. doi: 10.1007/s00261-016-0909-2
12. Dhanda S, Thakur M, Kerkar R, Jagmohan P. Diffusion-weighted imaging of gynecologic tumors: diagnostic pearls and potential pitfalls. *Radiographi*cs 2014; **34:** 1393-416. doi: 10.1148/rg.345130131
13. Jeong YY, Outwater EK, Kang HK. Imaging evaluation of ovarian masses. *Radiographics* 2000; **20:** 1445-70. doi: 10.1148/radiographics.20.5.g00se101445
14. El-Wekil A, Mohammad S Abdullah MS**,** El-Kholy SS. The role of MRI in the differentiation between benign and malignant ovarian lesions. *Menoufia Med J* 2017; **32:** 106-11. doi: 10.4103/mmj.mmj_548_17
15. Alt C, Bharwani N, Brunesch L, Danza FM, Derme M, El Sayed RF, et al. *ESUR quick guide to female pelvis imaging 1.0.* 2019: European Society of Urogenital Radiology. [cited 2020 May 15]. Available at: http://www.esur.org/fileadmin/content/2019/ESUR_2019_-_ESUR_Quick_Guide_to_Female_Pelvis_Imaging.pdf
16. Koc Z, Erbay G, Ulusan S, Seydaoglu G, Aka-Bolat F. Optimization of b value in diffusion-weighted MRI for characterization of benign and malignant gynecological lesions. *J Magn Reson Imaging* 2012; **35:** 650-9. doi: 10.1002/jmri.22871
17. Foti PV, Attinà G, Spadola S, Caltabiano R, Farina R, Palmucci S, et al. MR imaging of ovarian masses: classification and differential diagnosis. *Insights Imaging* 2016; **7:** 21-41. doi: 10.1007/s13244-015-0455-4
18. Meinhold-Heerlein I, Fotopoulou C, Harter P, Kurzeder C, Mustea A, Wimberger P, et al. The new WHO classification of ovarian, fallopian tube, and primary peritoneal cancer and its clinical implications. *Arch Gynecol Obstet* 2016; **293:** 695-700. doi: 10.1007/s00404-016-4035-8

19. Outwater EK, Siegelman ES, Hunt JL. Ovarian teratomas: tumor types and imaging characteristics. *Radiographics* 2001; **21:** 475-90. doi: 10.1148/radiographics.21.2.g01mr09475

20. Caruso PA, Marsh MR, Minkowitz S, Karten G. An intense clinicopathologic study of 305 teratomas of the ovary. *Cancer* 1971; **27:** 343-8. doi: 10.1002/1097-0142(197102)27:2<343::aid-cncr2820270215>3.0.co;2-b

21. Nakayama T, Yoshimitsu K, Irie H, Aibe H, Tajima T, Nishie A, et al. Diffusion-weighted echo-planar MR imaging and ADC mapping in the differential diagnosis of ovarian cystic masses: usefulness of detecting keratinoid substances in mature cystic teratomas. *J Magn Reson Imaging* 2005; **22:** 271-8. doi: 10.1002/jmri.20369

22. Agostinho L, Horta M, Salvador JC, Cunha TM. Benign ovarian lesions with restricted diffusion. *Radiol Bras* 2019; **52:** 106-11. doi: 10.1590/0100-3984.2018.0078

23. Feuerlein S, Pauls S, Juchems MS, Stuber T, Hoffmann MH, Brambs HJ, et al. Pitfalls in abdominal diffusion-weighted imaging: how predictive is restricted water diffusion for malignancy. *AJR Am J Roentgenol* 2009; **193:** 1070-6. doi: 10.2214/AJR.08.2093

24. Dunn DP, Kelsey NR, Lee KS, Smith MP, Mortele KJ. Non-oncologic applications of diffusion-weighted imaging (DWI) in the genitourinary system. *Abdom Imaging* 2015; **40:** 1645-54. doi: 10.1007/s00261-015-0471-3

25. Duarte AL, Dias JL, Cunha TM. Pitfalls of diffusion-weighted imaging of the female pelvis. *Radiol Bras* 2018; **51:** 37-44. doi: 10.1590/0100-3984.2016.0208

26. Takeuchi M, Matsuzaki K, Nishitani H. Diffusion-weighted magnetic resonance imaging of ovarian tumors: differentiation of benign and malignant solid components of ovarian masses. *J Comput Assist Tomogr* 2010; **34:** 173-6. doi: 10.1097/RCT.0b013e3181c2f0a2

27. Moyle PL, Kataoka MY, Nakai A, Takahata A, Reinhold C, Sala E. Nonovarian cystic lesions of the pelvis. *Radiographics* 2010; **30:** 921-38. doi: 10.1148/rg.304095706

28. Kim MY, Rha SE, Oh SN, Jung SE, Lee YJ, Kim YS, et al. MR Imaging findings of hydrosalpinx: a comprehensive review. *Radiographics* 2009; **29:** 495-507. doi: 10.1148/rg.292085070

29. Laurent PE, Thomassin-Piana J, Jalaguier-Coudray A. Mucin-producing tumors of the ovary: MR imaging appearance. *Diagn Interv Imaging* 2015; **96:** 1125-32. doi: 10.1016/j.diii.2014.11.034

30. Marko J, Marko KI, Pachigolla SL, Crothers BA, Mattu R, Wolfman DJ. Mucinous neoplasms of the ovary: radiologic-pathologic correlation. *Radiographics* 2019; **39:** 982-97. doi: 10.1148/rg.2019180221

31. Vargas HA, Barrett T, Sala E. MRI of ovarian masses. *J Magn Reson Imaging* 2013; **37:** 265-81. doi: 10.1002/jmri.23721

32. Jung SE, Lee JM, Rha SE, Byun JY, Jung JI, Hahn ST. CT and MR imaging of ovarian tumors with emphasis on differential diagnosis. *Radiographics* 2002; **22:** 1305-25. doi: 10.1148/rg.226025033

33. Cho SM, Byun JY, Rha SE, Jung SE, Park GS, Kim BK, et al. CT and MRI findings of cystadenofibromas of the ovary. *Eur Radiol* 2004; **14:** 798-804. doi: 10.1007/s00330-003-2060-z

34. Tang YZ, Liyanage S, Narayanan P, Sahdev A, Sohaib A, Singh N, et al. The MRI features of histologically proven ovarian cystadenofibromas-an assessment of the morphological and enhancement patterns. *Eur Radiol* 2013; **23:** 48-56. doi: 10.1007/s00330-012-2568-1

35. Siegelman ES, Outwater EK. Tissue characterization in the female pelvis by means of MR imaging. *Radiology* 1999; **212:** 5-18. doi: 10.1148/radiology.212.1.r99jl455

36. Woodward PJ, Sohaey R, Mezzetti TP Jr. Endometriosis: radiologic-pathologic correlation. *Radiographics* 2001; **21:** 193-216; questionnaire 288-94. doi: 10.1148/radiographics.21.1.g01ja14193

37. Rockall A, Forstner R. Adnexal diseases. In: Hodler J, Kubik-Huch RA, von Schulthess GK, editors. *Diseases of the abdomen and pelvis 2018-2021: diagnostic imaging.* Cham (CH): IDKD Book; 2018. p. 75-84.

38. Siegelman ES, Oliver ER. MR imaging of endometriosis: ten imaging pearls. *Radiographics* 2012; **32:** 1675-91. doi: 10.1148/rg.326125518

39. Imaoka I, Wada A, Kaji Y, Hayashi T, Hayashi M, Matsuo M, et al. Developing an MR imaging strategy for diagnosis of ovarian masses. *Radiographics* 2006; **26:** 1431-48. doi: 10.1148/rg.265045206

40. Zhang H, Zhang GF, He ZY, Li ZY, Zhang GX. Prospective evaluation of 3T MRI findings for primary adnexal lesions and comparison with the final histological diagnosis. *Arch Gynecol Obstet* 2014; **289:** 357-64. doi: 10.1007/s00404-013-2990-x

41. Funt SA, Hricak H. Ovarian malignancies. *Top Magn Reson Imaging* 2003; **14:** 329-37. doi: 10.1097/00002142-200308000-00005

42. Hussain SM, Outwater EK, Siegelman ES. MR imaging features of pelvic mucinous carcinomas. *Eur Radiol* 2000; **10:** 885-91. doi: 10.1007/s003300051029

43. Hann LE, Lui DM, Shi W, Bach AM, Selland DL, Castiel M. Adnexal masses in women with breast cancer: US findings with clinical and histopathologic correlation. *Radiology* 2000; **216:** 242-7. doi: 10.1148/radiology.216.1.r00jl15242

44. Outwater EK, Siegelman ES, Kim B, Chiowanich P, Blasbalg R, Kilger A. Ovarian Brenner tumors: MR imaging characteristics. *Magn Reson Imaging* 1998; **16:** 1147-53. doi: 10.1016/s0730-725x(98)00136-2

45. Yamashita Y, Hatanaka Y, Torashima M, Takahashi M, Miyazaki K, Okamura H. Characterization of sonographically indeterminate ovarian tumors with MR imaging. A logistic regression analysis. *Acta Radiol* 1997; **38:** 572-7. doi: 10.1080/02841859709174389

46. Bent CL, Sahdev A, Rockall AG, Singh N, Sohaib SA, Reznek RH. MRI appearances of borderline ovarian tumours. *Clin Radiol* 2009; **64:** 430-8. doi: 10.1016/j.crad.2008.09.011

47. deSouza NM, O'Neill R, McIndoe GA, Dina R, Soutter WP. Borderline tumors of the ovary: CT and MRI features and tumor markers in differentiation from stage I disease. *AJR Am J Roentgenol* 2005; **184:** 999-1003. doi: 10.2214/ajr.184.3.01840999

48. Maggino T, Gadducci A, D'Addario V, Pecorelli S, Lissoni A, Stella M, et al., Prospective multicenter study on CA 125 in postmenopausal pelvic masses. *Gynecol Oncol* 1994; **54:** 117-23. doi: 10.1006/gyno.1994.1179

49. Zhang H, Zhang GF, He ZY, Li ZY, Zhu M, Zhang GX. Evaluation of primary adnexal masses by 3T MRI: categorization with conventional MR imaging and diffusion-weighted imaging. *J Ovarian Res* 2012; **5:** 33. doi: 10.1186/1757-2215-5-33